International Symposium
On Turbulence and Shear Flow
Phenomena (TSFP-9)
June 30 - July 3, 2015 *Melbourne, Australia*

SETTLING OF HEATED PARTICLES IN HOMOGENEOUS TURBULENCE

Ari Frankel
Department of Mechanical Engineering
Stanford University
488 Escondido Mall, Building 500, Stanford, CA 94305
frankel1@stanford.edu

Hadi Pouransari
Department of Mechanical Engineering
Stanford University
488 Escondido Mall, Building 500, Stanford, CA 94305
hadip@stanford.edu

Filippo Coletti
Department of Aerospace Engineering and Mechanics
University of Minnesota
110 Union St SE, Akerman Hall, Minneapolis, MN 55455
fcoletti@umn.edu

Ali Mani
Department of Mechanical Engineering
Stanford University
488 Escondido Mall, Building 500, Stanford, CA 94305
alimani@stanford.edu

ABSTRACT

We consider the case of inertial particles heated by thermal radiation while settling by gravity through a turbulent transparent gas. Numerical simulations of forced homogeneous turbulence are performed taking into account the two-way coupling of both momentum and temperature between the dispersed and continuous phases. Particles much smaller than the smallest flow scales are considered and the point-particle approximation is adopted. The particle Stokes number (based on the Kolmogorov time scale) is of order unity, while the nominal settling velocity is up to an order of magnitude larger than the Kolmogorov velocity, marking a critical difference with previous two-way coupled simulations. It is found that non-heated particles enhance turbulence when their settling velocity is sufficiently high. When heated, particles shed plumes of buoyant gas, further modifying the turbulence structure. At the considered radiation intensities, clustering is strong but the classic mechanism of preferential concentration is modified, while preferential sweeping is eliminated or even reversed. Particle heating also causes a significant reduction of the mean settling velocity, which is caused by positively buoyant plumes in the vicinity of particle clusters. The downward drag force exerted by the particles on the fluid breaks the symmetry of the un-laden turbulence and increases the magnitude of the vertical velocity fluctuations in the unheated case. This asymmetry is reduced in the presence of radiative heating due the reduced falling speed of the heavier particles, where buoyancy effects counteract gravity and the preferential sweeping mechanism.

Introduction

Multiphase flows in which a dense dispersed phase interacts with a lighter carrier fluid are ubiquitous in nature and industrial applications. Often the fluid flow is in the turbulent regime, and the inertial particles cannot follow its rapid velocity fluctuations. This velocity lagging can lead to high local concentration in zones of high strain and away from vortex cores (Maxey, 1987; Squires & Eaton, 1991). This phenomenon, known as preferential concentration, has been widely investigated and is considered a critical mechanism for the growth of cloud droplets (Shaw, 2003) and the mixing of air and fuel in spray combustion (Sahu *et al.*, 2014).

For particles much denser than the carrier fluid and small compared to the flow scales, the relevant parameter describing the particle-fluid interaction is the Stokes num-

ber $\mathrm{St} = \tau_p/\tau_f$, the ratio between the aerodynamic response time of the particle and the fluid time scale. When the latter is taken as the Kolmogorov scale τ_η, the maximum level of preferential concentration is typically found at $\mathrm{St}_\eta \approx 1$ (Wang & Maxey, 1993).

Turbulence can increase the settling velocity of small inertial particles beyond the nominal terminal velocity V_t in a quiescent fluid because trajectories that sample the downward side of the eddies are favored. This mechanism, referred to as preferential sweeping, was first demonstrated in homogeneous isotropic turbulence by Wang & Maxey (1993). Measurements from Aliseda *et al.* (2002) and Yang & Shy (2005) confirmed this effect, which is especially strong when $\mathrm{St}_\eta \approx 1$ and $V_t/u' \approx 0.5$, u' being the root-mean-square fluid velocity fluctuation (Yang & Lei, 1998).

In the present study we explore the behavior of heated particles settling through homogeneous turbulence and the interaction between dispersed and continuous phases. The physical parameters are chosen to be representative of a dilute, optically thin mixture of air and solid particles subject to thermal radiation. The particle Stokes number is chosen to produce significant preferential concentration. Numerical simulations are performed taking into account the two-way coupling of both momentum and temperature between the dispersed and continuous phase. Since particles much smaller than the smallest flow scales are considered, all relevant spatio-temporal scales can be resolved.

Methodology

Governing equations

The compressible low-Mach Navier-Stokes equations for a fluid of constant viscosity μ are

$$\frac{\partial \rho}{\partial t} + \frac{\partial \rho u_j}{\partial x_j} = 0 \tag{1}$$

$$\frac{\partial \rho u_i}{\partial t} + \frac{\partial \rho u_i u_j}{\partial x_j} = -\frac{\partial p}{\partial x_i} + \frac{\partial \tau_{ij}}{\partial x_j} + \rho g_i - \sum_{n=1}^{N_p} \frac{m_p}{\tau_p}(u_i - v_{i,n})\delta(x_i - y_{i,n}), \tag{2}$$

where u_i are the velocity components, t is time, x_i are the spatial coordinates, p is the hydrodynamic pressure, τ_{ij} is the Newtonian viscous stress tensor, ρ is the fluid density, g_i ($i = 3$) is the gravitational acceleration, δ_{ij} is the Kronecker delta, N_p is the number of particles in an Eulerian cell, and $v_{i,n}$ and $y_{i,n}$ are the velocity and spatial coordinates of the n-th particle. We consider spherical Stokesian particles with mass and aerodynamic response time $m_p = \rho_p \pi D_p^3/6$ and $\tau_p = \rho_p D_p^2/18\mu$, respectively, with ρ_p being the particle density. The fluid is considered to be an ideal gas of constant thermal conductivity k and heat capacities C_v and C_p (at constant volume and pressure, respectively), for which the energy equation reads

$$\frac{\partial}{\partial t}(\rho C_v T_f) + \frac{\partial}{\partial x_j}(\rho C_p T_f u_j) = k\frac{\partial^2 T_f}{\partial x_j \partial x_j} + \sum_{n=1}^{N_p} \pi D_p^2 h (T_{p,n} - T_f)\delta(x_i - y_{i,n}), \tag{3}$$

where T_f is the fluid temperature, $T_{p,n}$ is the temperature of the n-th particle and h is the convective heat transfer coefficient, which for a Stokesian particle can be calculated from the Nusselt number $\mathrm{Nu} = hD_p/k = 2$. The gas properties reflect those of air at ambient temperature and pressure.

Particles are individually tracked along their trajectories, according to the simplified particle equation of motion, where only contributions from Stokes drag and gravity are retained,

$$\frac{dy_i}{dt} = v_i \qquad \frac{dv_i}{dt} = \frac{u_i - v_i}{\tau_p} + g_i. \tag{4}$$

Under the Stokesian particle assumption, the terminal velocity of the particles is $V_t = g\tau_p$. Each particle is subject to a radiative heat flux I_o. The carrier phase is transparent to radiation, whereas the incident radiative flux on each particle is completely absorbed. Because we focus on relatively small volume fractions, the fluid-particle medium is considered optically thin. Under these hypotheses, the direction of the radiation is inconsequential, each particle receives the same radiative heat flux, and its temperature T_p is governed by

$$\frac{d}{dt}(m_p C_{v,p} T_p) = \frac{\pi D_p^2}{4} I_o - \pi D_p^2 h (T_p - T_f) \tag{5}$$

where $C_{v,p}$ is the particle specific heat.

Numerical implementation

Each of the above equations is solved using a staggered grid formulation and second-order central differences. Both the fluid and particle equations are integrated in time using a fourth order Runge-Kutta time integrator. Eulerian quantities are evaluated at the location of the particles using linear interpolation, and coupling from the particle to the fluid is performed with linear projection to the nearest fluid volumes. The turbulence is maintained using a linear forcing method (Lundgren, 2003). The domain is a triply periodic cube with length L_b, which is discretized in N^3 points to resolve the Kolmogorov scale. For the one-way coupled simulation without radiation, in which the flow scales are predicted by homogeneous isotropic turbulence theory, $N = 256$. The fluid is considered an ideal gas, with constant dynamic viscosity and an initial density of ρ_o at a temperature of T_o. The mean fluid momentum is set to zero in each time step, which is equivalent to applying a mean hydrostatic pressure gradient to the fluid. This is necessary to prevent the fluid from accelerating continuously in vertical direction, due to the drag imposed by the settling particles and the buoyancy (Bosse *et al.*, 2005). Similarly, the mean temperature of the fluid is artificially set to be constant, to prevent the fluid from warming up indefinitely. Therefore the velocity and temperature dynamics investigated in this study have to be considered fluctuations around a potentially time-varying mean.

Physical Parameters

The main parameters describing the turbulent fluid phase and the dispersed particle phase for the performed simulations are listed in Table 1. The values are representative of the system after it has become stationary (typically

after five eddy turnover times). A baseline case with no radiation and one-way coupled particle transport is used for comparison. Because of the anisotropy caused by the two-way coupling, we define as the velocity and length scale of the large eddies, respectively,

$$u' = \sqrt{2/3\mathrm{TKE}} = \sqrt{2u_{\mathrm{rms}}^2/3 + w_{\mathrm{rms}}^2/3} \qquad L = u'^3/\varepsilon \qquad (6)$$

where $\mathrm{TKE} = 1/2(2u_{rms}^2 + w_{rms}^2)$ is the turbulent kinetic energy, u_{rms} and w_{rms} are the rms fluctuations of the horizontal and vertical components, and ε is the turbulent dissipation rate. The hydrodynamic forcing is the same for all cases, and produces a microscale Reynolds number $\mathrm{Re}_{\lambda,\Phi_v=0} = 65$ in the one-way coupled regime ($\Phi_v = 0$ subscript denotes no mass loading). In every case the particle diameter is assumed to be $D_p = 40\ \mu$m, which results in $D_p/\eta \lesssim 0.1$ and $\mathrm{Re}_p \lesssim 1$, confirming the validity of the point-particle approximation. The volume fraction is $\Phi_v = 10^{-5}$ (corresponding to a mass fraction Φ_m between 1% and 10%), which is considered in the two-way coupled regime (Elghobashi, 1994). The momentum transfer from the heavy particles and the buoyancy-driven plumes strongly modify the turbulence structure, as evident for example from the changes in Re_λ between the various cases. The change in turbulent scales also alters the effective Stokes number. The level of radiation is associated with a steady state particle temperature increase with respect to the surrounding fluid, which from equation 5 is

$$T_p - T_o = \frac{D_p I_o}{8k} \qquad (7)$$

where $\mathrm{Nu} = hD_p/k = 2$ has been substituted, which is valid for spherical particles at the present Re_p range. The particle-to-fluid temperature ratio is 1.3 for the intermediate and 2.2 for the higher radiation level.

Results

Settling of non-heated particles

Particle clustering For all considered cases, the particle Stokes number indicates that strong turbulence clustering is expected. This is confirmed by analyzing the probability density function (PDF) of the volumes of the Voronoi cells around each particle, which are defined based on the distance to the neighboring particles. The Voronoi cell size distribution is commonly used to recognize the presence of clusters/voids, i.e. regions of significantly higher/lower concentration with respect to the spatial average over the entire domain (Monchaux *et al.*, 2010). Figure 1 shows the PDF of Voronoi cells normalized by the average volume $\langle V \rangle$. The PDFs for the inertial particles are much broader than the Γ distribution expected for randomly distributed particles (Tagawa *et al.*, 2012), which is a hallmark of turbulence clustering. The variance of the Voronoi cell volumes, which is often used to quantify the degree of clustering (Monchaux *et al.*, 2010), is maximum for the intermediate density ratio ($\rho_p/\rho_o = 4166$), which is expected since for this case the Stokes number is closer to unity ($St_\eta = 1.6$).

Momentum coupling Here we consider particles of significant settling velocities compared to both the small- and large-scale turbulent velocity fluctuations, and we find that the turbulence intensity is enhanced by the faster settling particles. This is clearly illustrated in Figure 2, that displays values of TKE and ε normalized by their correspondent levels in the one-way coupled case, $\mathrm{TKE}_{\Phi_v=0}$ and $\varepsilon_{\Phi_v=0}$. For $\rho_p/\rho_o = 833$, which corresponds to settling velocities of the same order as the turbulent velocity scales (see Table 1), the turbulent energy and dissipation rate are slightly smaller than those in the one-way coupled flow, in agreement with previous findings (Bosse *et al.*, 2006). However, for heavier particles with settling parameters $V_t/u_\eta = \mathcal{O}(10)$, both TKE and ε increase by an order of magnitude due to the momentum two-way coupling.

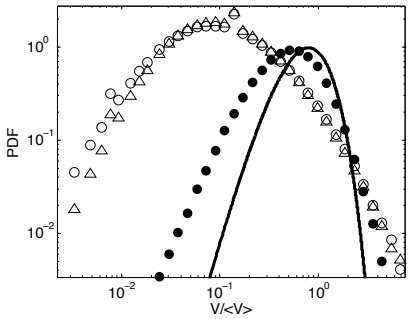

Figure 1. Voronoi volume distributions for the particles with different density ratios, full circles: $\rho_p/\rho_o = 833$, open circles: $\rho_p/\rho_o = 4166$, triangles: $\rho_p/\rho_o = 8333$, line: Γ distribution.

This increase of turbulent agitation with particle density cannot be attributed to the loading, since the turbulent energy has been shown to decrease with increasing mass loading in stationary turbulence (Squires & Eaton, 1991; Boivin *et al.*, 1998). This cause is rather to be found in the drag forces exerted by the quickly settling particles, which alter the turbulence structure: as the particle falls, the lost gravitational potential energy is input to the fluid. This picture is consistent with the results of the simulations of Elghobashi & Truesdell (1993) for decaying turbulence. Our results suggest that rapidly settling, point-like particles falling through forced stationary turbulence enhance turbulence intensity.

Settling velocity Figure 3 shows the fractional variation of particle settling velocity with respect to the theoretical terminal velocity in quiescent air. In agreement with previous studies, the increase in settling rate ranges between 20% and 35% when normalized by the nominal terminal velocity (Yang & Shy, 2005; Bosse *et al.*, 2006). The result for the one-way coupled case ($\rho_p/\rho_o = 833$, $St_\eta = 0.18$) is also shown. Depending on the normalization, the latter reads $(W_p - V_t)/u_\eta = 0.32$ or $(W_p - V_t)/u' = 0.083$, in excellent agreement with the results obtained in similar regimes by Wang & Maxey (1993); Good *et al.* (2014) respectively.

In the two-way coupled cases the increase in settling velocity is more pronounced for higher density ratios. The trend is the same whether the change in settling velocity is normalized by V_t or by u'. This is consistent with results of Bosse *et al.* (2006), who found a monotonic increase in settling rate with increasing mass loading. They described this behavior as a consequence of the collective particle drag

	One-way	Two-way									
		No radiation			Radiation						
Run #	0	1	2	3	4	5	6	7	8	9	10
ρ_p/ρ_o	833	833	4166	8333	833	833	4166	8333	833	4166	8333
Φ_m	0.01	0.01	0.05	0.1	0.01	0.01	0.05	0.1	0.01	0.05	0.1
Re_λ	65	62	104	153	57	68	93	109	63	105	129
St_η	0.18	0.17	1.6	5.1	0.16	0.24	1.48	3.4	0.37	2.7	5.8
V_t/u'	0.47	0.49	1.37	1.84	0.51	0.40	1.50	2.62	0.30	1.05	1.87
V_t/u_η	1.84	1.91	6.75	10.68	2.0	1.64	7.17	13.91	1.28	5.34	10.43
T_p/T_o	1	1	1	1	1.006	1.3	1.3	1.3	2.21	2.21	2.21

Table 1. Physical parameters and main flow statistics.

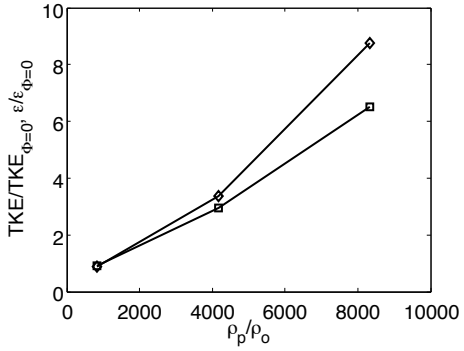

Figure 2. Dependence of the TKE (squares) and dissipation (diamonds) on particle bulk density of the two-way coupled simulations relative to a one-way coupled simulation. The increased TKE and dissipation at higher mass loading indicates the transfer of gravitational potential energy from the particles to the surrounding fluid.

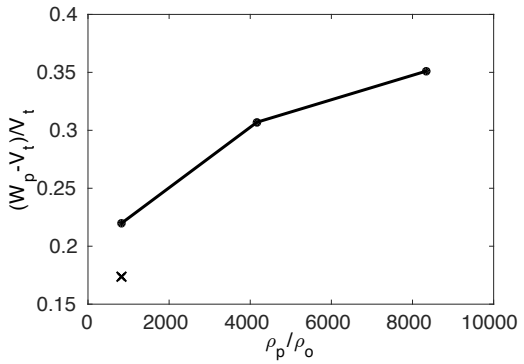

Figure 3. The settling parameter for the various particle densities with respect to the theoretical terminal velocity (line), and the respective one-way coupled result (cross mark).

that enhances the downward fluid motion. However, in the present regime, another mechanism may produce this result. The heavier particles release more potential energy into the fluid, leading to substantially higher turbulence intensity (Figure 2). A more elevated Re_λ is known to produce faster settling (Yang & Lei (1998) among others). Although the latter trend was demonstrated most clearly in one-way coupled cases, it was also reported in two-way coupled regimes by Yang & Shy (2005).

Settling of heated particles

Particle distribution The PDF of Voronoi cell volumes in Figure 4 confirms that the particles are strongly clustered. Again the particles with St_η closer to unity (see Table 1) display more intense clustering, as evident from the long tails of the distributions.

In homogeneous turbulence the mechanism of preferential concentration causes the inertial particles to be in regions of low enstrophy and high strain (Squires & Eaton, 1991). This is confirmed also for the considered flow in Figure 5, that displays the joint PDF of normalized particle concentration C/C_o and fluid enstrophy ξ/ξ_o, where ξ is the fluid enstrophy. Here C_o is the domain-averaged concentration and ξ_o is the average enstrophy in the one-way coupled, unheated case. In all considered cases higher concentration levels are found in regions of low enstrophy. However, both particle density and heating have significant effects. The heavier particles (whose settling velocity largely exceeds the Kolmogorov velocity) tend to sample the flow more homogeneously. This is true despite the fact that Re_λ substantially increases with particle density (see Table 1). The reason for the more uniform distribution of heavier particles may be twofold. On one hand the relatively high settling velocity de-correlates the particle position from the regions of high strain and low enstrophy. On the other hand, the strong momentum two-way coupling alters the structure of the turbulence, which modifies the classic picture of preferential concentration.

The introduction of radiative heat has a similar effect, in that the particles become more uniformly distributed with respect to the enstrophy field. This is attributed to the turbulence modification. As it will be discussed later, the particles release heat into the surrounding fluid, producing low density and positively buoyant plumes, which in turn modify the turbulent flow field.

In the presence of gravity, according to the picture of preferential sweeping proposed by Wang & Maxey (1993), the inertial particles sample downward regions more often than upward regions of the turbulent flow. This is true for all considered non-heated cases, as shown in Figure 6 by

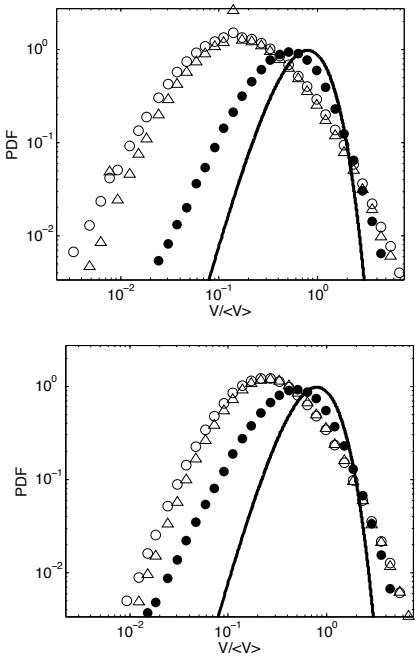

Figure 4. Voronoi volume distributions for the particles with different density ratios, full circles: $\rho_p/\rho_o = 833$, open circles: $\rho_p/\rho_o = 4166$, triangles: $\rho_p/\rho_o = 8333$, line: Γ distribution.

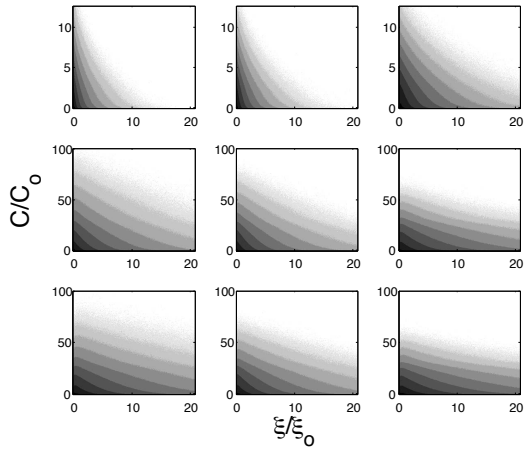

Figure 5. The logarithmically-scaled joint probability density functions of normalized concentration and enstrophy. From left to right: $T_p/T_o = 1$, $T_p/T_o = 1.3$, $T_p/T_o = 2.2$. From top to bottom: $\rho_p/\rho_o = 833$, $\rho_p/\rho_o = 4166$, $\rho_p/\rho_o = 8333$. Grayscale contour levels are equally spaced (arbitrary units).

the joint PDF of particle concentration C and fluid vertical velocity W (normalized by u'). Also, the two-way momentum coupling causes the fluid near the heavy particles to be dragged downward even faster (Bosse *et al.*, 2006), increasing the probability of finding particles in regions $W < 0$. However, in the presence of heating, the trend is reversed, and the particles are more likely to be found in regions of upward turbulent fluctuations. This is again a hint of the

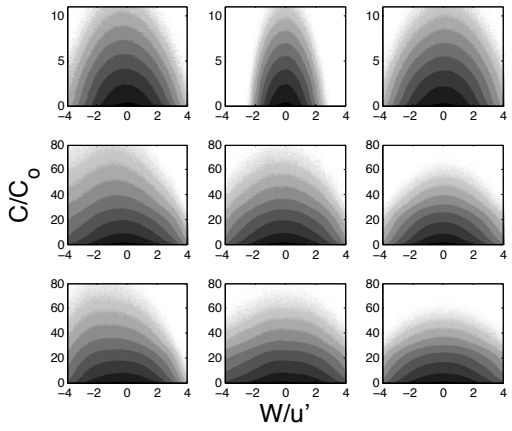

Figure 6. The logarithmically-scaled joint probability density functions of normalized concentration and vertical velocity. From left to right: $T_p/T_o = 1$, $T_p/T_o = 1.3$, $T_p/T_o = 2.2$. From top to bottom: $\rho_p/\rho_o = 833$, $\rho_p/\rho_o = 4166$, $\rho_p/\rho_o = 8333$. Grayscale contour levels are equally spaced (arbitrary units).

presence of positively buoyant plumes shed by the hot particles. It is also apparent that for the non-heated cases the range of vertical fluid velocities gets broader for more massive particles, which reflects the increased turbulence activity.

Settling velocity Figure 7 presents the difference between the mean settling velocity and the nominal terminal velocity as a function of the particle-to-fluid temperature ratio. In order to highlight the impact on the particle-turbulence interaction, we normalize the velocity difference by u' (normalization using u_η as the fluid velocity scale leads to a similar result). For all density ratios the heating of the particles hinders the falling speed. We remark that this is not a consequence of a global upward fluid velocity, since the mean velocity is set to zero at every time step. It is rather caused by the high temperature regions around the particles (and especially the particle clusters), which produce localized updraft in correspondence of the high particle concentration areas. At the most intense radiation level this effect offsets the preferential sweeping mechanism, and the falling speed is lower than the nominal terminal velocity in a quiescent fluid.

Interestingly, the heavier particles reduce their falling speed more than the lighter particles. A possible reason is that the heavier particles are more densely clustered (see Figures 1 and 4) and the clusters generate larger and more intense buoyant plumes, hindering the settling. Another likely reason is that the buoyancy production term in the turbulent kinetic energy transport is larger for particles of greater mass.

Turbulence anisotropy Figure 8 demonstrates that particle heating augments the anisotropy in the $\rho_p/\rho_o = 833$ case, but reduces it for the higher density ratios. This is because heating reduces the falling speed of heavier particles more sharply. This limits the particle momentum transfer to the flow, and in turn lessens anisotropy and turbulence enhancement.

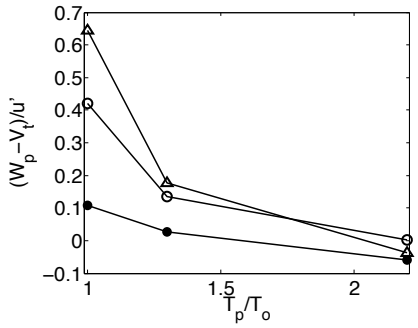

Figure 7. Plot of the settling parameter for each of the different particle densities for different heating levels, Voronoi volume distributions for the particles with different density ratios, full circles: $\rho_p/\rho_o = 833$, open circles: $\rho_p/\rho_o = 4166$, triangles: $\rho_p/\rho_o = 8333$.

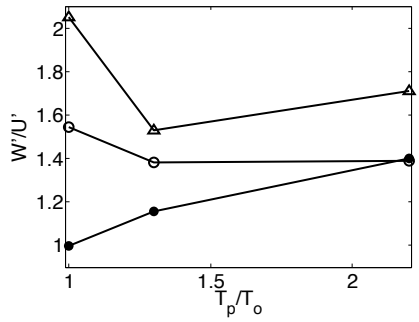

Figure 8. Ratio of the root-mean-square vertical and horizontal velocities as a function heating level for each of the different particle densities, full circles: $\rho_p/\rho_o = 833$, open circles: $\rho_p/\rho_o = 4166$, triangles: $\rho_p/\rho_o = 8333$.

Conclusions

We investigated solid particles falling through homogeneous air turbulence while heated by thermal radiation. In the considered optically thin regime, radiation is simply modeled as an equal heat flux input to each particle. Particles much smaller than the Kolmogorov scale are considered, which permits the solution for all relevant flow scales taking into account both the momentum and thermal coupling between phases. In the considered range of particle density and heating levels the Stokes number indicates strong preferential concentration, and the settling velocity is comparable to the fluid velocity fluctuations. The imposed mass loading is sufficient to cause sizable modification of the air turbulence, and the maximum radiation level more than doubles the absolute temperature of the particles.

Clustering is intense for particles with $St_\eta = \mathcal{O}(1)$, regardless of momentum or temperature coupling. However, the mechanism of preferential concentration in high-strain/low-vorticity regions is blurred by the turbulence modification. In the absence of radiation, particles with $V_t/u_\eta \approx 1$ experience substantial increase in their settling velocity due to preferential sweeping, as expected from previous studies. Settling of heavier particles ($V_t/u_\eta > 1$) augments the turbulent energy and increases the vertical fluid velocity fluctuations with respect to the horizontal component. In the presence of radiation, hot buoyant plumes are shed from the heated particles, which reduces the settling velocity. The preferential sweeping mechanism breaks down and particles do not preferentially sample regions of downward moving fluid. Heating reduces the settling velocity of heavier particles more substantially.

REFERENCES

Aliseda, A., Cartellier, A., Hainaux, F. & Lasheras, J. 2002 Effect of preferential concentration on the settling velocity of heavy particles in homogeneous isotropic turbulence. *J. Fluid Mech.* **468**, 77–105.

Boivin, M., Simonin, O. & Squires, K. 1998 Direct numerical simulation of turbulence modulation by particles in isotropic turbulence. *J. Fluid Mech.* **375**, 235–263.

Bosse, T., Kleiser, L., Hartel, C. & Meiburg, E. 2005 Numerical simulation of finite reynolds number suspension drops settling under gravity. *Phys. Fluids* **17**, 037101.

Bosse, T., L., Kleiser & Meiburg, E. 2006 Small particles in homogeneous turbulence: Settling velocity enhancement by two-way coupling. *Phys. Fluids* **18**, 027102.

Elghobashi, S. 1994 On predicting particle-laden turbulent flows. *Appl. Sci. Res.* **52**, 309–329.

Elghobashi, S. & Truesdell, G. 1993 On the two-way interaction between homogeneous turbulence and dispersed solid particles. 1: Turbulence modification. *Phys. Fluids* **5**, 1790–1801.

Good, G., Ireland, P., Bewley, G., Bodenschatz, E., Collins, L. & Warhaft, Z. 2014 Settling regimes of inertial particles in isotropic turbulence. *J. Fluid Mech.* **759**, R3.

Lundgren, T. 2003 Linearly forced isotropic turbulence. In *Annual Research Briefs*, pp. 461–473. Center for Turbulence Research, Stanford University.

Maxey, M 1987 The gravitational settling of aerosol particles in homogeneous turbulence and random flow fields. *J. Fluid Mech.* **174**, 441–465.

Monchaux, R., Bourgoin, M. & Cartellier, A. 2010 Preferential concentration of heavy particles: A voronoi analysis. *Phys. Fluids* **22**, 103304.

Sahu, S., Hardalupas, Y. & Taylor, A. 2014 Droplet-turbulence interaction in a confined polydispersed spray: effect of droplet size and flow length scales on spatial droplet-gas velocity correlations. *J. Fluid Mech.* **741**, 98–138.

Shaw, R. 2003 Particle-turbulence interactions in atmospheric clouds. *Annu. Rev. Fluid Mech.* **35**, 183–227.

Squires, K. & Eaton, J. 1991 Particle response and turbulence modification in isotropic turbulence. *Phys. Fluids A* **2**, 1191.

Tagawa, Y., Mercado, J., Prakash, V., Calzavarini, E., Sun, C. & Lohse, D. 2012 Three-dimensional lagrangian moroni analysis for clustering of particles and bubbles in turbulence. *J. Fluid Mech.* **693**, 201–215.

Wang, L. & Maxey, M. 1993 Settling velocity and concentration distribution of heavy particles in homogeneous isotropic turbulence. *J. Fluid Mech.* **371**, 179–205.

Yang, C. & Lei, U. 1998 The role of the turbulent scales in the settling velocity of heavy particles in homogeneous isotropic turbulence. *J. Fluid Mech.* **371**, 179–205.

Yang, T. & Shy, S. 2005 Two-way interaction between solid particles and homogeneous air turbulence: particle settling rate and turbulence modification measurements. *J. Fluid Mech.* **526**, 171–216.